On the stability of equilibria with unorthodox q(r) profiles to the resistive internal kink mode

1989 Plasma Phys. Control. Fusion 31 1127

(http://iopscience.iop.org/0741-3335/31/7/008)

Plasma Physics and Controlled Fusion, Vol. 31, No. 7, pp. 1127 to 1140, 1989
Printed in Great Britain.
0741-3335/89 $3.00+ .00
IOP Publishing Ltd. and Maxwell Pergamon Macmillan plc

ON THE STABILITY OF EQUILIBRIA WITH UNORTHODOX $q(r)$ PROFILES TO THE RESISTIVE INTERNAL KINK MODE*

R. FITZPATRICK
Culham Laboratory, Abingdon, Oxon OX14 3DB, U.K.
(Euratom/UKAEA Fusion Association)

(*Received* 1 *August* 1988; *and in revised form* 2 *February* 1989)

Abstract—The linear resistive-MHD layer equations are solved numerically for the internal kink mode and the dispersion relation is obtained. We consider two rather unorthodox types of $q(r)$ profile, both of which have zero shear at the layer; i.e.

(i) non-monotonic $q(r)$ with a minimum value lying just above unity,
(ii) monotonic $q(r)$ with a point of inflection at $q = 1$.

One interesting feature of our results for both types of $q(r)$ profile is the appearance of overstable solutions for certain parameter ranges. For class (i), we find that the mode becomes first overstable and then purely growing as the minimum value of $q(r)$ decreases. For realistic plasma parameters the band of overstability is thin, but non-negligible. For class (ii), we find that for realistic plasma parameters the mode is completely stable.

1. INTRODUCTION

IN A RECENT PAPER dealing with the trigger mechanism for "sawtooth" collapses in Tokamaks, HASTIE *et al.* (1987) emphasized the importance of obtaining reliable growth rates close to marginal stability for the resistive "internal" kink mode (this mode is generally believed to be responsible for the initial displacement of the plasma core observed in a sawtooth collapse). Two rather unorthodox classes of $q(r)$ profile (where q is the safety factor) were found to be especially significant in this context; namely

(i) non-monotonic $q(r)$ with a minimum value just above unity at $r = r_1$,
(ii) monotonic $q(r)$ for which $q(r_1) = 1$, and $r = r_1$ is a point of inflection of q.

Numerical results from a linear toroidal resistive-MHD code (FAR) indicated that these profiles could be stable to resistive $m = 1, n = 1$ modes under certain conditions, and moreover could yield very large growth rates close to the marginal stability boundary. This last result is very interesting since, up to now, it has been difficult to account for the rapidity of the initial plasma displacement in a sawtooth collapse using the standard model, in which the equilibrium evolves resistively through some marginal stability boundary for the $m = 1$, $n = 1$ mode. The problem is that the growth rates which are obtained close to marginality, for orthodox $q(r)$ profiles, are usually far too small to account for the observations.

In this paper we solve the linear resistive-MHD layer equations for the internal kink mode, using the two previously mentioned classes of $q(r)$ profile. The approach is analogous to that of COPPI *et al.* (1976), who obtained analytic solutions for $q(r)$ profiles with finite shear at the layer. We hope to be able to confirm the previously

mentioned numerical results, especially the prediction of large growth rates close to marginality. For the second class of $q(r)$ profile, the results from FAR rather surprisingly indicated that the $m = 1$, $n = 1$ resistive mode could become overstable for certain ranges of parameters—we also hope to be able to gain some insight into this effect. In our analysis we shall make use of the low β, large aspect ratio orderings. Our results should be applicable to both cylindrical and toroidal equilibria, provided that the appropriate expression for δW is used (see later).

2. PRELIMINARY ANALYSIS

By analogy with COPPI *et al.* (1976), the general linearized $m = 1$, $n = 1$ resistive layer equations for a thin layer in the limit of small β and large aspect ratio are:

$$\rho \frac{d^2\xi}{dx^2} = \frac{1}{\gamma^2}\left\{F(x)\frac{d^2 iB_{1r}}{dx^2} - \frac{d^2F(x)}{dx^2}(iB_{1r})\right\}, \tag{1}$$

$$iB_{1r} = -F(x)\xi + \frac{\eta}{\gamma r_1^2}\frac{d^2 iB_{1r}}{dx^2}, \tag{2}$$

where

$$x = \frac{(r-r_1)}{r_1}, \tag{3}$$

and

$$F = \frac{B_\theta}{r}(1-q). \tag{4}$$

Here, r_1 is the radial coordinate of the centre of the layer, ρ the density, ξ the plasma displacement, γ the growth rate, η the resistivity and B_{1r} the perturbed radial field. In the following, R is the major radius, ε the inverse aspect ratio, and S the magnetic Reynolds number. The resistive layer solution is matched to the outer ideal solution by imposing the following boundary conditions on equations (1) and (2):

$$\begin{aligned} &\xi \to \xi_\infty; \quad \frac{d\xi}{dx} \to \frac{\xi_\infty}{r_1^2 F^2(x)}\int_0^{r_1} g(r)\,dr \quad \text{on inner edge of layer,} \\ &\xi \to 0; \quad \frac{d\xi}{dx} \to \frac{\xi_\infty}{r_1^2 F^2(x)}\int_0^{r_1} g(r)\,dr \quad \text{on outer edge of layer,} \end{aligned} \tag{5}$$

where the function $g(r)$ is defined in COPPI *et al.* (1976).

Now, in cylindrical geometry, the change in potential energy of the system due to the zero-order plasma displacement ξ_∞ can be written

$$\delta W = 2\pi^2 R|\xi_\infty|^2 B_\phi^2\left(\frac{r_1}{R}\right)^4 \delta W^{(C)}, \tag{6}$$

where

$$\delta W^{(C)} = -\int_0^{r_1} \frac{dr}{r_1}\left(\frac{r}{r_1}\right)^3\left(\frac{1}{q}-1\right)\left(\frac{1}{q}+3\right), \tag{7}$$

for zero β. It can easily be shown that

$$\int_0^{r_1} g(r)\,dr \equiv B_\phi^2\left(\frac{r_1}{R}\right)^4 \delta W^{(C)}. \tag{8}$$

Clearly, the layer solution is completely determined, from equations (1), (2), (5) and (8), once $\delta W^{(C)}$ [which is a function of the $q(r)$ profile outside the layer] is specified.

It is well known that the expression for δW in toroidal geometry is completely different to that for cylindrical geometry given above—this is because the leading-order cylindrical contribution to δW, which is $O(\varepsilon^2)$ and usually dominates the expression, is exactly cancelled out by a corresponding toroidal term for an $m = 1$, $n = 1$ mode. Thus, in toroidal geometry the relatively simple expression $\delta W^{(C)}$ must be replaced by a far more complicated term $\delta W^{(T)}$, which is detailed in BUSSAC *et al.* (1975). The layer solution itself is independent of the geometry of the system once the appropriate expression ($\delta W^{(C)}$ or $\delta W^{(T)}$) is substituted in equation (8) to determine the boundary conditions.

3. NON-MONOTONIC $q(r)$ PROFILES WITH $q'(r_1) = 0$

3.1. *Introduction*

Consider a plasma with the $q(r)$ distribution sketched in Fig. 1. We can expand $F(x)$ in the vicinity of the layer as follows:

$$F(x) = -\tfrac{1}{2}(B_\theta q'' r)_{r=r_1}(x^2+h^2), \tag{9}$$

where

$$h^2 = \frac{\delta q}{(\frac{1}{2}q''r^2)_{r=r_1}}. \tag{10}$$

Substitution of the above into (1) and (2) yields the appropriate layer equations:

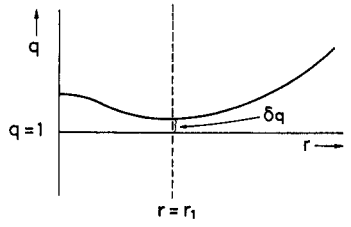

FIG. 1.—A typical type (i) $q(r)$ profile.

$$\frac{d^2\xi}{dx^2} = \frac{1}{\lambda^2}\left(\tfrac{1}{2}(x^2+h^2)\frac{d^2\psi}{dx^2} - \psi\right), \tag{11}$$

$$\psi = -\tfrac{1}{2}(x^2+h^2)\xi + \frac{S^{-1}}{\lambda}\frac{d^2\psi}{dx^2}, \tag{12}$$

where $\psi = -iB_{1r}/(B_\theta q'' r)_{r=r_1}$ and $\lambda = \gamma\tau_A^*$. Here the Alfvén* time-scale (cf. KADOMTSEV, 1975) is given by $\tau_A^* = r_1/\{(B_\theta/\sqrt{\rho})(q''r^2)\}_{r=r_1}$, and the magnetic Reynolds number is defined as $S = (r_1^2/\eta)/\tau_A^*$. Substitution of (9) into equations (5) gives the layer boundary conditions:

$$\begin{aligned} &\xi \to \xi_\infty; \quad x^4\frac{d\xi}{dx} \to -\frac{\xi_\infty \lambda_H}{\pi} \quad \text{on inner edge of layer,} \\ &\xi \to 0; \quad x^4\frac{d\xi}{dx} \to -\frac{\xi_\infty \lambda_H}{\pi} \quad \text{on outer edge of layer,} \end{aligned} \tag{13}$$

where

$$\lambda_H = \frac{4\pi(r_1/R)^2}{(q''r^2)^2_{r=r_1}}[-\delta W^{(C,T)}]. \tag{14}$$

The ordering which makes every term in (11) and (12) comparable is

$$\psi/\xi \sim \lambda \sim x^2 \sim h^2 \sim S^{-1/2}. \tag{15}$$

Normalizing with respect to this ordering yields the following form for the resistive layer equations:

$$\frac{d^2\xi}{d\hat{x}^2} = \frac{1}{\hat{\lambda}^2}\left\{\tfrac{1}{2}(\hat{x}^2+\hat{h}^2)\frac{d^2\hat{\psi}}{d\hat{x}^2} - \hat{\psi}\right\}, \tag{16}$$

$$\hat{\psi} = -\tfrac{1}{2}(\hat{x}^2+\hat{h}^2)\xi + \frac{1}{\hat{\lambda}}\frac{d^2\hat{\psi}}{d\hat{x}^2}, \tag{17}$$

where $\psi = S^{-1/2}\hat{\psi}$, $x = S^{-1/4}\hat{x}$ etc. Information about the external solution (via the boundary condition) now enters in the normalized variables through the quantity $\hat{\lambda}_H$ defined by $\lambda_H = S^{-3/4}\hat{\lambda}_H$.

The ideal layer equations can be solved analytically to give the following dispersion relation

$$\lambda_H = \{2[4\lambda^2+h^4]([4\lambda^2+h^4]^{1/2}+h^2)\}^{1/2}. \tag{18}$$

This has a marginal stability boundary at

$$\lambda_H = 2h^3 \propto \delta q^{3/2}, \tag{19}$$

thus agreeing with HASTIE *et al.* (1987).

Unlike the standard case considered by COPPI *et al.* (1976), the present problem is far too complex to solve analytically; we must therefore resort to a numerical approach. In the following, we shall employ the two-point boundary value technique of Lentini and Pereyra, in which the boundary conditions are simultaneously specified at $\hat{x} = 0$ and $\hat{x} = B$ (where $B \gg 1$), and the intermediate solution then obtained by a finite-difference algorithm.

After making allowances for the possibility of complex growth rates, we can reduce our problem to a system of eight first-order differential equations. Appropriate normalizations and symmetry arguments easily yield six boundary conditions at $\hat{x} = 0$. The remaining two boundary conditions hold at $x = B$ and are obtained from the asymptotic expansion of equations (16) and (17), always taking care to choose only physically acceptable solutions. Finally, the eigenvalue $\hat{\lambda}$ is fixed in the complex plane by the requirement that $\hat{\lambda}_H$ be real.

3.2. *Numerical results*

First, let us consider the results for which the mode is purely growing; these are displayed in Figs 2(a–c). Note that:

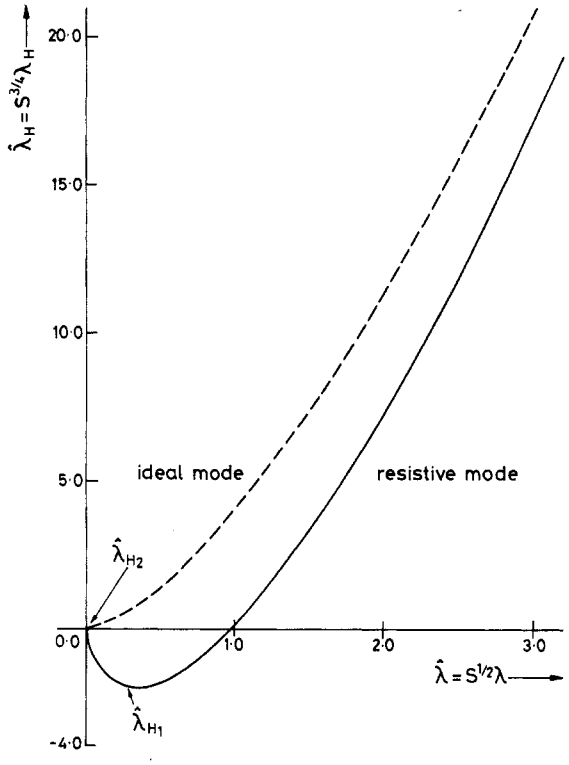

FIG. 2(a).—The purely growing branches of the ideal and resistive dispersion relations, calculated for a type (i) $q(r)$ profile with $\hat{h} = 0.0$.

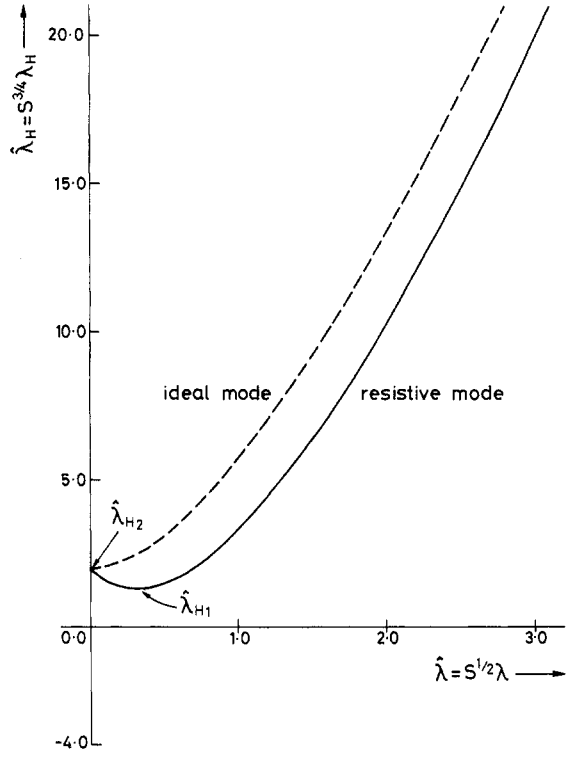

FIG. 2(b).—The purely growing branches of the ideal and resistive dispersion relations, calculated for a type (i) $q(r)$ profile with $\hat{h} = 1.0$.

(a) for $\lambda_H \gg S^{-3/4}$, the resistive growth rate approaches the ideal growth rate asymptotically;
(b) for $\lambda_H \sim S^{-3/4}$, the resistive mode has a correspondingly greater growth rate than the ideal mode—both modes having comparable growth rates;
(c) the ideal mode is stabilized when λ_H falls below a critical value

$$\lambda_{H2} = 2h^3. \tag{20}$$

However, the purely growing resistive mode is only stabilized when λ_H falls below λ_{H1}, where it is always found that $\lambda_{H1} < \lambda_{H2}$. Note that $\lambda_{H2} - \lambda_{H1} \sim O(S^{-3/4})$, with both values increasing rapidly with increasing h.

The behaviour of λ_H as a function of λ in Figs 2(a–c), in particular the minimum for $\lambda \neq 0$, strongly points to the existence of an overstable resistive mode for $\lambda_H < \lambda_{H1}$, with $\lambda_H = \lambda_{H1}$ the point of bifurcation into the complex plane.

The numerical results for which the growth rate is complex are displayed in Figs 3(a–c). (In fact, since the solutions for the growth rate occur in complex conjugate pairs, only one half of the complex plane is shown.) Note that:

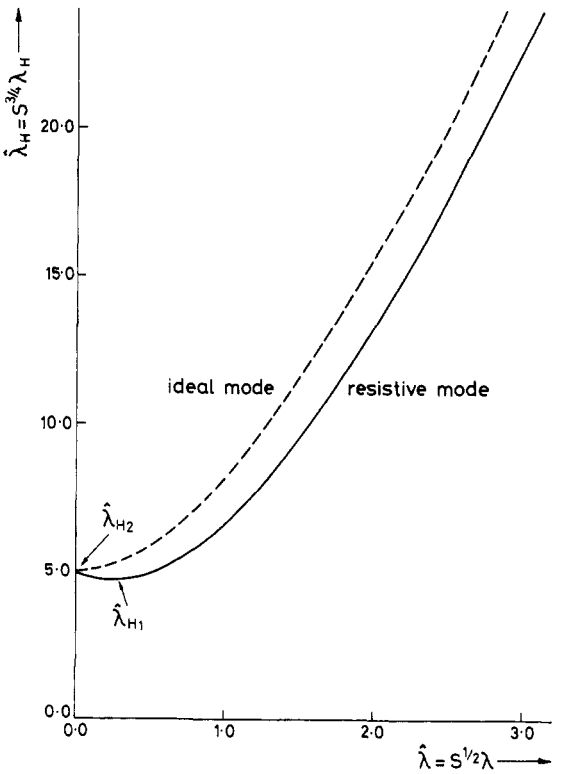

FIG. 2(c).—The purely growing branches of the ideal and resistive dispersion relations, calculated for a type (i) $q(r)$ profile with $\hat{h} = \sqrt[3]{2.5}$.

(a) there is indeed an overstable resistive mode for values of λ_H lying below λ_{H1}, with $\lambda_H = \lambda_{H1}$ the point of bifurcation of the solution;
(b) there exists a critical λ_H (denoted λ_{H0}) below which the overstable resistive mode is damped. At $\lambda_H = \lambda_{H0}$ the mode is marginally stable and oscillatory.

The behaviour of $\hat{\lambda}_{H0}$, $\hat{\lambda}_{H1}$ and $\hat{\lambda}_{H2}$ as functions of $2\hat{h}^3$ is shown in Fig. 4.

4. MONOTONIC $q(r)$ PROFILES WITH $q'(r_1) = q''(r_1) = 0$

4.1. *Introduction*

Suppose now that the $q(r)$ distribution is as sketched in Fig. 5. We can expand $F(x)$ in the vicinity of the layer as follows:

$$F(x) \simeq -\tfrac{1}{6}(B_\theta q''' r^2)_{r=r_1} x^3. \tag{21}$$

Substitution of the above into (1) and (2) yields the new layer equations:

$$\frac{d^2\xi}{dx^2} = \frac{1}{\lambda^2}\left\{\tfrac{1}{6}x^3\frac{d^2\psi}{dx^2} - x\psi\right\}, \tag{22}$$

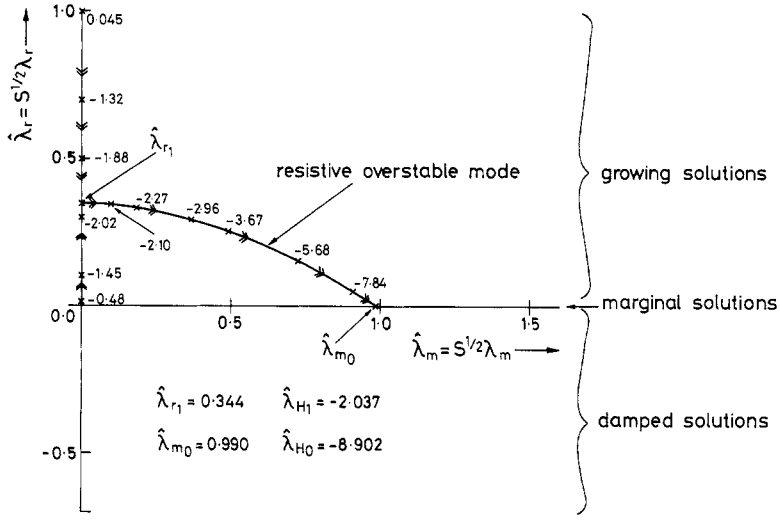

FIG. 3(a).—The overstable branch of the resistive dispersion relation, calculated for a type (i) $q(r)$ profile with $\hat{h} = 0.0$. λ_r is the real part of the growth rate, with λ_m the imaginary part. Values of $\hat{\lambda}_H$ are given at various points. The arrows indicate the direction of decreasing $\hat{\lambda}_H$.

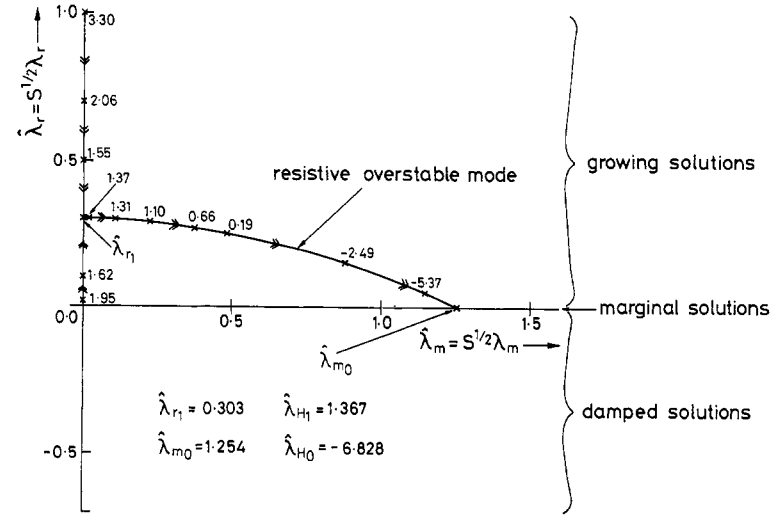

FIG. 3(b).—The overstable branch of the resistive dispersion relation, calculated for a type (i) $q(r)$ profile with $\hat{h} = 1.0$.

$$\psi = -\tfrac{1}{6}x^3\xi + \frac{S^{-1}}{\lambda}\frac{\mathrm{d}^2\psi}{\mathrm{d}x^2}, \tag{23}$$

where $\psi = -iB_{1r}/(B_\theta q''' r^2)_{r=r_1}$ and $\tau_A^* = r_1/\{(B_\theta/\sqrt{\rho})(q''' r^3)\}_{r=r_1}$.

The new layer boundary conditions are

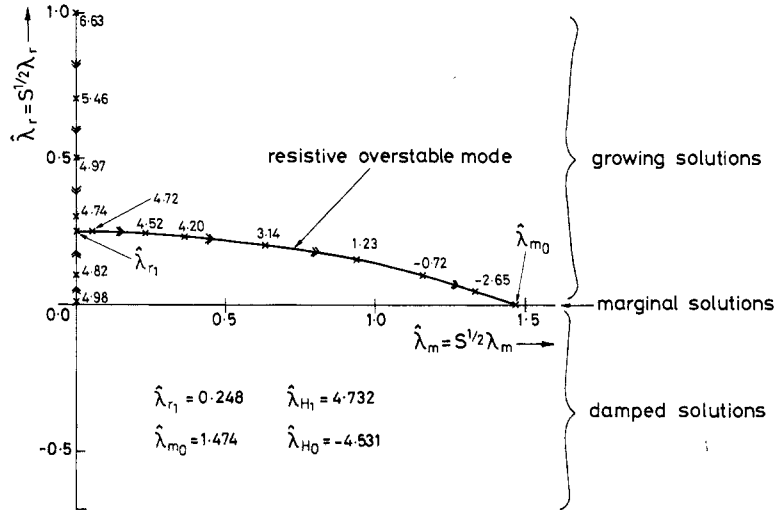

FIG. 3(c).—The overstable branch of the resistive dispersion relation, calculated for a type (i) $q(r)$ profile with $\hat{h} = \sqrt[3]{2.5}$.

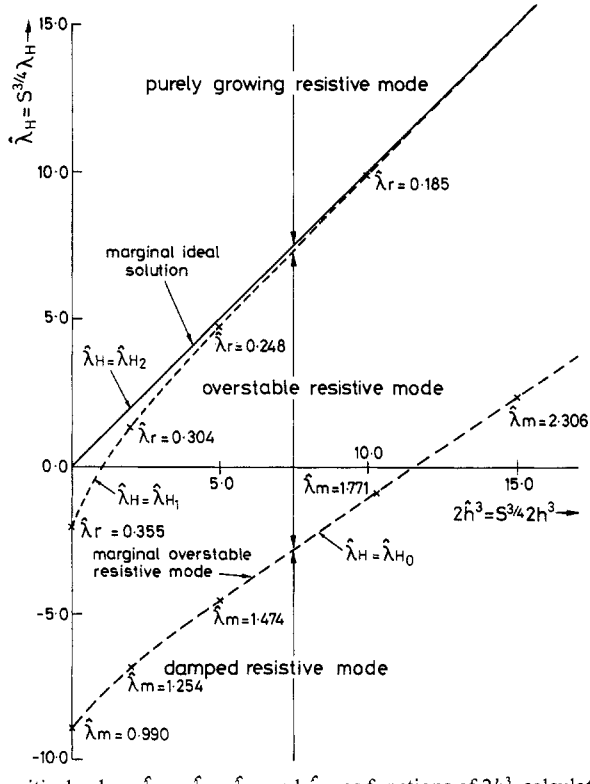

FIG. 4.—The critical values $\hat{\lambda}_H = \hat{\lambda}_{H0}$, $\hat{\lambda}_{H1}$ and $\hat{\lambda}_{H2}$ as functions of $2h^3$, calculated for type (i) $q(r)$ profiles.

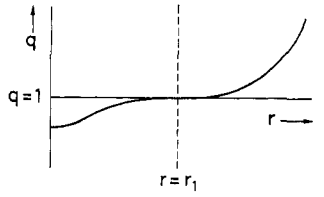

FIG. 5.—A typical type (ii) $q(r)$ profile.

$$\xi \to \xi_\infty ; \quad x^6 \frac{d\xi}{dx} \to -\frac{\xi_\infty \lambda_H}{\pi} \quad \text{on inner edge of layer,}$$

$$\xi \to 0 ; \quad x^6 \frac{d\xi}{dx} \to -\frac{\xi_\infty \lambda_H}{\pi} \quad \text{on outer edge of layer,} \tag{24}$$

where

$$\lambda_H = \frac{36\pi (r_1/R)^2}{(q''' r^3)^2_{r=r_1}} [-\delta W^{(C,T)}]. \tag{25}$$

The ordering which makes every term in (22) and (23) comparable is

$$\psi/\xi \sim \lambda \sim x^3 \sim S^{-3/5} ; \tag{26}$$

hence the normalized layer equations can be written,

$$\frac{d^2\xi}{d\hat{x}^2} = \frac{1}{\hat{\lambda}^2} \left\{ \tfrac{1}{6} \hat{x}^3 \frac{d^2\hat{\psi}}{d\hat{x}^2} - \hat{x}\hat{\psi} \right\}, \tag{27}$$

$$\hat{\psi} = -\tfrac{1}{6} \hat{x}^3 \xi + \frac{1}{\hat{\lambda}} \frac{d^2\hat{\psi}}{d\hat{x}^2}. \tag{28}$$

Note that asymptotic matching to the external solution now appears through the quantity $\hat{\lambda}_H$ defined by $\lambda_H = S^{-1}\hat{\lambda}_H$.

The following analytic ideal dispersion relation can easily be obtained from the layer equations after the neglect of the resistive term;

$$\lambda_H = \tfrac{3}{2} |6\lambda|^{5/3}. \tag{29}$$

4.2. *Numerical results*

The layer equations can be solved numerically using an analogous technique to that discussed in the previous section. The results obtained for the case of a purely growing mode are displayed in Fig. 6. Note that:

(a) for $\lambda_H \gg S^{-1}$, the resistive growth rate approaches the ideal growth rate asymptotically;

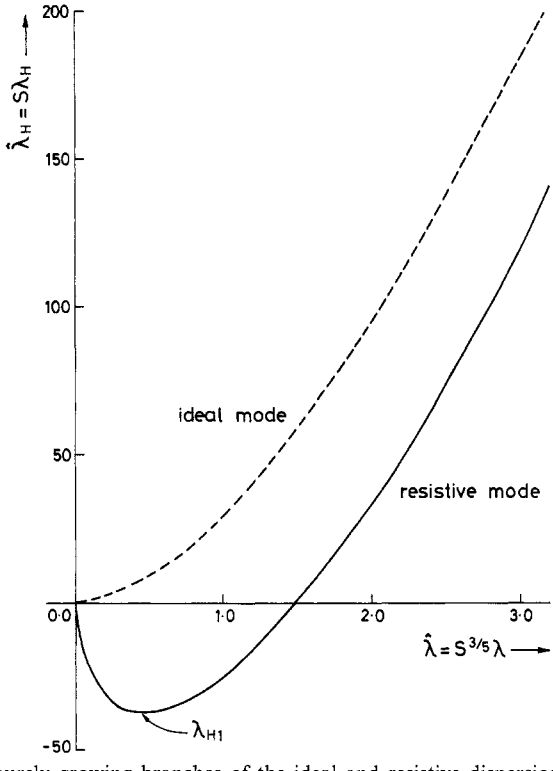

FIG. 6.—The purely growing branches of the ideal and resistive dispersion relations, calculated for a type (ii) $q(r)$ profile.

(b) for $\lambda_H \sim S^{-1}$, the resistive mode has a correspondingly greater growth rate than the ideal mode—both modes having comparable growth rates;
(c) the ideal mode is stabilized when λ_H falls below zero, and the purely growing resistive mode disappears when λ_H falls below λ_{H1}, where $\lambda_{H1} < 0$. Note that $\lambda_{H1} \sim O(S^{-1})$.

The results obtained for the case of a complex growth rate are displayed in Fig. 7. Note that:

(a) there is again an overstable resistive mode for values of λ_H lying below λ_{H1}, with $\lambda_H = \lambda_{H1}$ the point of bifurcation of the solution;
(b) there exists a critical λ_H (denoted λ_{H0}) below which the overstable resistive mode is damped. At $\lambda_H = \lambda_{H0}$ the mode is marginally stable and oscillatory. Once again this result differs markedly from that finite shear layer theory of COPPI *et al.*, where resistive instability is predicted for all λ_H, and is therefore inevitable if the axial value of q is less than unity.

5. CONCLUSIONS

5.1. *Non-monotonic* q(r) *with* $q'(r_1) = 0$

There are many reasons for believing that this type of $q(r)$ profile may actually occur in a real discharge. One argument is as follows: immediately after a sawtooth

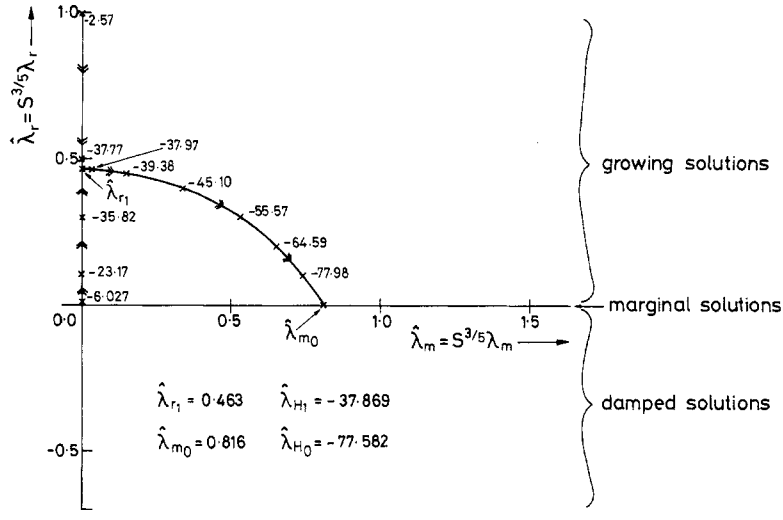

FIG. 7.—The overstable branch of the resistive dispersion relation, calculated for a type (ii) $q(r)$ profile. λ_r is the real part of the growth rate, with λ_m the imaginary part. Values of $\hat{\lambda}_H$ are given at various points. The arrows indicate the direction of decreasing $\hat{\lambda}_H$.

collapse $q(r)$ should be raised above unity everywhere and the temperature profile centrally flattened (assuming reconnection has taken place). The consequent large temperature gradients at the inversion radius give rise to enhanced transport there, which should eventually lead to a local minimum in q. The whole $q(r)$ profile will subsequently evolve downwards (i.e. δq will decrease) on a resistive timescale, as a result of Ohmic heating. Note, however, that non-monotonic $q(r)$ profiles are possible even if reconnection does not take place, as has been shown by some recent transport simulations, e.g. PARAIL and PEREVERZEV (1980); PFEIFFER (1985) and DENTON *et al.* (1987).

In a standard Tokamak the poloidal beta is often small; we would therefore expect $\delta W^{(T)} < 0$ ($\lambda_H > 0$) for a toroidal equilibrium in which $q > 1$ everywhere. It follows that the ideal mode is stable, provided δq lies above a critical value,

$$\delta q_c^{(i)} = \frac{1}{2^{1/3}(q''r^2)_{r=r_1}^{1/3}}\left[-\pi\left(\frac{r_1}{R}\right)^2\delta W^{(T)}\right]^{2/3}. \tag{30}$$

For realistic equilibria $\delta q_c^{(i)}$ is quite small ($\delta q_c^{(i)} \sim 0.01$, say). By the time δq has evolved resistively to zero the ideal growth rate will have risen to a value

$$\gamma_c\Big/\left(\frac{1}{\tau_A^*}\right) = \frac{1}{(q''r^2)_{r=r_1}^{1/3}}\left[-\pi\left(\frac{r_1}{R}\right)^2\delta W^{(T)}\right]^{2/3} \equiv 2^{1/3}\delta q_c^{(i)}, \tag{31}$$

which under realistic conditions is fairly substantial. It is clear that for this type of $q(r)$ profile a small decrease in δq of order 0.01 can cause the rapid onset of the ideal instability.

Once resistivity is taken into account we find that as δq is decreased the mode

becomes first overstable and then purely unstable. The boundary between overstability and pure growth occurs at $\delta q = \delta q_c^{(r)}$. Note that $\delta q_c^{(r)}$ approaches $\delta q_c^{(i)}$ as $S \to \infty$. The overstable resistive mode grows when $\delta q_c^{(r)} < \delta q < \delta q_c^{(o)}$, where (from Fig. 4) $\delta q_c^{(o)}$ is well approximated by

$$\delta q_c^{(o)} = \frac{1.28}{2^{1/3}(q''r^2)_{r=r_1}^{1/3}} \left[-\pi \left(\frac{r_1}{R}\right)^2 \delta W^{(T)} + 2.0(q''r^2)_{r=r_1}^2 S^{-3/4} \right]^{2/3}. \tag{32}$$

In the limit as $S \to \infty$, $\delta q_c^{(o)} \to 1.28 \delta q_c^{(i)}$; thus we obtain the significant result that, as δq is decreased, the band of overstability preceding the pure growth of the mode is of non-negligible thickness for all values of S. In fact, as $S \to \infty$ the overstable resistive mode transforms into an ideal oscillatory mode, with the real part of the growth rate become vanishingly small. We conclude that for large S ($S \sim 10^8$, say) the characteristic rapid switch-on of the mode, as δq is decreased slightly, is unaffected. For smaller S ($S < 10^5$, say), however, the onset of the mode will be preceded by a broad band of overstability.

5.2. *Monotonic* q(r) *with* $q'(r_1) = q''(r_1) = 0$

A $q(r)$ profile with a point of inflexion at $q = 1$ was introduced by HASTIE *et al.* (1987) in order to attempt an explanation of the TEXTOR $q(r)$ observations in which $q(0) < 1$ throughout the whole sawtooth cycle—however it must be admitted that such a profile is fairly unlikely to ever occur in a real discharge. It is, nevertheless, a very interesting result that by a slight flattening of the $q(r)$ profile around $q = 1$, an equilibrium that under realistic conditions ($\delta W^{(T)} > 0$, $\lambda_H < 0$) would have been unstable to either a resistive internal kink mode or a tearing mode can be stabilized at high enough S. In fact, the resistive internal kink mode is stable when $S > S_c$, where

$$S_c = 77.6 \frac{(q'''r^3)_{r=r_1}^2}{36\pi(r_1/R)^2 \delta W^{(T)}}. \tag{33}$$

Thus, under realistic conditions a $q(r)$ profile with a point of inflection at $q = 1$ is completely stable to resistive $m = 1$, $n = 1$ modes.

5.3. *Discussion*

Using just the linearized resistive-MHD equations, we have found that the absence of shear across the "inner" layer [i.e. $q'(r_1) = 0$] leads to the appearance of an overstable mode for certain ranges of $\delta W^{(T)}$, and the disappearance of the tearing mode limit as $\delta W^{(T)} \to \infty$. It is, as yet, unclear whether or not these results will persist for more realistic layer dynamics.

The Bussac expression $\delta W^{(T)}$ takes into account the fact that in toroidal geometry there is a small $m = 2$, $n = 1$ harmonic associated with an $m = 1$, $n = 1$ displacement eigenfunction. If, however, we allow for finite resistivity at the $q = 2$ surface (assuming, of course, that it lies within the plasma) then poloidal coupling occurs between the $m = 1$ and $m = 2$ models, and the situation is greatly complicated (BUSSAC *et al.*, 1977; CONNOR *et al.*, 1988). Note that this effect will only produce significant deviations from the results quoted in this paper if the shear around the $q = 1$ surface is very small.

REFERENCES

BUSSAC M. N., EDERY D., PELLAT R. and SOULE J. L. (1977) *Plasma Physics and Controlled Nuclear Fusion Research* 1976. *Proc. 6th International Conf.*, Berchtesgaden (IAEA, Vienna, 1977), Vol. 1, p. 607.

BUSSAC M. N., PELLAT R., EDERY D. and SOULE J. L. (1975) *Phys. Rev. Lett.* **35**, 1638.

CONNOR J. W., COWLEY S. C., HASTIE R. J. *et al.* (1988) *Physics Fluids* **31**, 577.

COPPI B., GALVAO R., PELLAT R., ROSENBLUTH M. N. and RUTHERFORD P. H. (1976) *Sov. J. Plasma Phys.* **2**, 533.

DENTON R. E., DRAKE J. F. and KLEVA R. G. 1987) *Physics Fluids* **30**, 1448.

HASTIE R. J., HENDER T. C. *et al.* (1987) *Physics Fluids* **30**, 1756.

KADOMTSEV B. B. (1975) *Sov. J. Plasma Phys.* **1**, 389.

PARAIL V. V. and PEREVERZEV G. V. (1980) *Sov. J. Plasma Phys.* **6**, 14.

PFEIFFER W. (1985) *Nucl. Fusion* **25**, 673.